T. Kaneko

Color Composite Pictures from Principal Axis Components of Multispectral Scanner Data

Abstract: When principal axis transformations are applied to multispectral scanner (MSS) data, the majority of data variability is shown to be contained in the first two or three components. This paper describes a method for generating a color composite picture from these components whereby most of the information collected by an MSS can be conveyed in a single color picture. The first component is found to be a weighted sum of image data from all channels, and therefore it is natural to associate the first component with brightness. To be consistent with this interpretation, only the first component of the transformed data is used to control the brightness of the color composite picture.

Introduction

Photographic film has been the primary medium for remote sensing [1]; however, there are two major drawbacks [2] to its use. First, photographic film has a limited spectral response in the region from the near ultraviolet to the near infrared. Second, conversion to electric signals is required for both telemetry and further machine processing. Consequently, non-photographic sensors such as electromagnetic scanners [called multispectral scanners (MSS)], and radar imaging devices have appeared. Examples of MSS are LANDSAT I and II (4 channels), the University of Michigan M7 scanner (12 channels), and the Skylab S192B (13 channels). The LANDSAT I and II MSS launched by NASA have been the most significant in demonstrating the capability of MSS to the remote-sensing community.

Although MSS data are readily adaptable to telemetry and machine processing, they must first be converted to images for human interpretation. These images are usually in the form of a set of black-and-white "pictures" (one for each of the spectral channels) or a color composite picture made from image data from three selected channels. The term "picture" will be used to refer to any interpretable form of image: photographic film, photographic prints, or TV display. Color pictures have a distinct advantage over their black-and-white counterparts since millions of different colors can be distinguished by the human eye while at most 200 different (gray level) shades are recognizable [3]. This paper describes a technique for making color composite pictures from MSS data such that these pictures contain more information than is normally found in the three channels usually selected.

Recent analyses have shown that the dimensionality of the MSS data is smaller than the number of channels, even though each channel occupies a non-overlapping spectral region. For example, LANDSAT four-channel image data are very well represented by two-dimensional data [4–6]. Even for the 13-channel S192B Skylab MSS, the first three variables of a principal axis transformation with the largest data variability represent almost all of the data variability [7, 8]. Therefore, if the three principal axis components with the largest data variability are used to make color pictures, the resulting pictures will contain most of the information collected by the MSS.

It has been shown by Ready and Wintz [9] that the first two to three principal axis components from the LARS six-channel MSS can convey practically all of the information. Fontanel et al. [10] and Santisteban and Munoz [11] have proposed color display methods based on individually controlling each of the blue, green, and red guns with the first three principal components. As a consequence, the brightness (for instance) of the resulting imagery depends upon all three components.

The first component is usually a weighted sum of all the bands that are reflective (i.e., visible to near-infrared bands from 0.4–1.5 μm) because the bands are positively correlated to one another. Since each MSS band measures incoming energy, it is natural to associate a weighted sum of MSS bands with brightness representing "energy." In order to be consistent with this interpretation, the method to be presented in this paper uses only the first component of the transformed data to control the brightness of the color composite picture.

Description of new method

- *Principal axis analysis and property of the first component*

A multispectral scanner (MSS) measures energy through spectral windows generally contained in the region between 0.3 μm (ultraviolet) and 16 μm (far infrared). Such spectral windows are called bands or channels; the latter term is used in this paper.

Let $X = (x_1, x_2, \cdots, x_n)$ denote the response of an n-channel MSS, where x_i is the ith channel response. Thus, the transformation of X into its principal axis components, $Y = (y_1, y_2, \cdots, y_n)$, is given by

$$Y = AX,$$

where $A = \{a_{ij}\}$ is an n by n matrix, and $y_1, y_2, \cdots, y_n$ are listed in the order of decreasing magnitude of data variability. For calculating A, see for example [12].

The problem with which we are concerned is that of finding a method for generating a color composite picture from the first two components $\{y_1\}$ and $\{y_2\}$ when the dimensionality of the MSS data is two, or from the first three components $\{y_1\}$, $\{y_2\}$, and $\{y_3\}$ of Y, where $\{\ \}$ is used to indicate the entire picture elements (pixels) of a given image.

Consider the first component, y_1. It is written as

$$y_1 = a_{11}x_1 + a_{12}x_2 + \cdots + a_{1n}x_n, \qquad (1)$$

where the coefficients satisfy the condition

$$a_{11}^2 + a_{12}^2 + \cdots + a_{1n}^2 = 1.$$

An important property of these coefficients is that they are all non-negative; i.e., $a_{1j} \geq 0$. This property seems to hold for any MSS image of natural objects in reflective bands (0.4–1.5 μm). In other words, band-to-band correlation is generally positive in these bands. Because of this, it is reasonable to say that the first component represents brightness [5].

This conclusion leads to a basic guideline for methods of generating color pictures from the transformed data: brightness of color pictures should be governed by the y_1 component alone. For example, a method for controlling the three color components red, green, and blue with y_1, y_2, and y_3 would yield color pictures inconsistent with this interpretation of the transformed data.

- *Mathematical representation of color*

Human visual perception of color is very complex. In this paper we define color as the mixture of three colors, red,

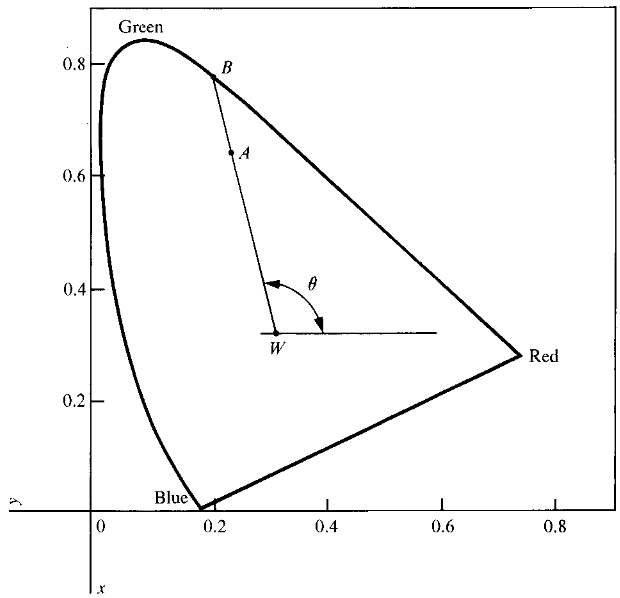

Figure 1 Hue and saturation defined on a chromaticity diagram.

green, and blue [3]. This definition is not unreasonable, and color pictures are made according to this principle. On a color TV display, color is realized by controlling the biases of three color guns. On a color photographic film converter the beam intensity of a cathode ray tube (CRT) is modulated for each of the three colors to expose the corresponding tripack color film.

In this paper it is assumed that the level of brightness on the TV display or on the tripack color film is proportional to the bias of the CRT, and also that the color is generated in an additive fashion. When the bias levels of the red, green, and blue guns are denoted by p_1, p_2, and p_3, respectively, the color H is then represented by

$$H = p_1\mathbf{r} - p_2\mathbf{g} + p_3\mathbf{b}, \qquad (2)$$

where $\mathbf{r}$, $\mathbf{g}$, and $\mathbf{b}$ are basis vectors for red, green and blue, respectively. For convenience, p_1, p_2, and p_3 are restricted to a range of 0 to 1, where 0 and 1 represent the minimum (zero) and maximum brightness, respectively:

$$0 \leq p_1, p_2, p_3 \leq 1.$$

Another representation of Eq. (2) is

$$H = B(q_1\mathbf{r} + q_2\mathbf{g} + q_3\mathbf{b}). \qquad (3)$$

Therefore, we have

$$B = p_1 + p_2 + p_3,$$

and

$$q_i = p_i/B \qquad i = 1, 2, 3.$$

Brightness is represented by B, and q_1, q_2, and q_3 (trichromatic coefficients) represent the relative magnitudes of red, green, and blue brightness levels, respectively. Since q_3 is dependent on both q_1 and $q_2 (q_3 = 1 - q_1 - q_2)$, the color H can be identified by the triplet (q_1, q_2, B). In particular, the (q_1, q_2) represent the x and y coordinates on a chromaticity diagram [3]. Such a diagram is a convenient way to introduce the terms hue and saturation. (Brightness, hue, and saturation are three independent values of color.) The angle θ and ratio WA/WB in Fig. 1 identify hue and saturation, respectively. Roughly speaking, hue corresponds to the dominant wavelength of the electromagnetic radiation emitted or reflected by the object and may be understood as a value used to differentiate yellow from red, for instance. Saturation, on the other hand, is a value used to differentiate purity of color: for example, pink (low saturation) from red (high saturation).

- *Formulation of new method*

For color H, as represented in Eq. (3), we would like the brightness B to be controlled by the principal component (y_1) having the largest data variability. Therefore, B is expressed as

$$B = f_0(y_1), \tag{4}$$

where f_0 is a function to be determined.

Next, consider a functional relationship of q_1 with y_1, y_2, and y_3. In Eq. (3) it is observed that when the blue, green, and red guns are controlled by p_1, p_2, and p_3, the hue and saturation are uniquely determined by the ratios of p_1, p_2, and p_3. More specifically, the values of q_1 and q_2 do not change when kp_1, kp_2, and kp_3 are substituted for p_1, p_2, and p_3, where k is a positive, real value. To maintain this property in the proposed method, q_1 and q_2 are controlled by y_2/y_1 and y_3/y_1, respectively. Thus, we have

$$q_1 = f_1(y_2/y_1),$$

and

$$q_2 = f_2(y_3/y_1). \tag{5}$$

Consequently, a color picture will be generated by

$$p_1 = f_0(y_1) f_1(y_2/y_1), \tag{6a}$$

$$p_2 = f_0(y_1) f_2(y_3/y_1), \tag{6b}$$

and

$$p_3 = f_0(y_1) \{1 - f_1(y_2/y_1) - f_2(y_3/y_1)\}. \tag{6c}$$

The functions $f_0(\ )$, $f_1(\ )$, and $f_2(\ )$ are chosen to be linear [13]:

$$f_0(y_1) = \alpha_0 y_1 + \beta_0, \tag{7a}$$

$$f_1(y_2/y_1) = \alpha_1 y_2/y_1 + \beta_1, \tag{7b}$$

and

$$f_2(y_3/y_1) = \alpha_2 y_3/y_1 + \beta_2. \tag{7c}$$

The coefficients α_0, α_1, α_2, β_0, β_1, and β_2 are constrained to satisfy the inequalities

$$0 \leq p_1, p_2, p_3 \leq 1, \tag{8}$$

where p_1, p_2, and p_3 are given in Eq. (6).

Procedures for determining α_i and β_i

- *Principal axis transformation for LANDSAT MSS data*

LANDSAT subframes consisting of 117 scan lines by 196 pixels are used to illustrate the method for determining values α_i and β_i in the linear functions described above. These subframes (extracted from LANDSAT full frames) cover ground areas of approximately $9 \times 11\ km^2$.

As was shown by Johnson [4], Kauth and Thomas [5] (transform for LANDSAT I), and Wheeler and Misra [6], the first two components of LANDSAT, selected in the order of magnitude of data variability, represent most of that variability. The transform given by Kauth and Thomas for LANDSAT II imagery is as follows:

$$y_1 = 0.334x_1 + 0.603x_2 + 0.676x_3 + 0.263x_4, \tag{9a}$$

$$y_2 = -0.283x_1 - 0.661x_2 + 0.577x_3 - 0.389x_4, \tag{9b}$$

$$y_3 = -0.900x_1 + 0.428x_2 - 0.076x_3 - 0.041x_4, \tag{9c}$$

and

$$y_4 = 0.404x_1 - 0.039x_2 - 0.505x_3 + 0.762x_4. \tag{9d}$$

Kauth and Thomas call the first, second, third, and fourth components "brightness," "greenness," "yellowness," and "non-such" components, respectively, based on their connotation with observed phenological growth patterns. To illustrate the method presented, we first consider two components, y_1 and y_2, for generating color pictures; then we consider three components, y_1, y_2, and y_3, that are computed by the above transformation.

In color infrared photography it is customary to use red to indicate vegetation (green); therefore, the second component y_2, indicating "greenness," controls the red component of color pictures. Thus, a pixel with a larger "greenness" value is tinted more reddish (i.e., assigned a higher saturation level of red), and q_1, which represents the proportion of red, is controlled by y_2/y_1:

$$q_1 = \alpha_1 y_2/y_1 + \beta_1. \tag{10}$$

This is in agreement with Eq. (7b).

- *Image generation by y_1 and y_2*

In this method, when the first two components alone are used to generate color pictures, the blue and green are set equal:

$$p_2 = p_3, \tag{11a}$$

or

$$q_2 = q_3 = 1/2(1 - q_1). \tag{11b}$$

The coefficients α_0 and β_0 in Eq. (7a) are determined from a histogram of the brightness component y_1 for a given image. First, the mean μ and the standard deviation σ are computed from the histogram. The range 6σ, from $(\mu - 3\sigma)$ to $(\mu + 3\alpha)$, is considered to be the total range of brightness. The coefficients α_0 and β_0 are determined by a linear transform that maps $(\mu - 3\sigma)$, μ, and $(\mu + 3\sigma)$ to B' $(1 - e)$, B', and B' $(1 + e)$, respectively. The average brightness of the resulting picture is indicated by B'; that is, B' equals the average of $(p_1 + p_2 + p_3)$, and e is described below. Therefore, the coefficients α_0 and β_0 are given as

$$\alpha_0 = \frac{eB'}{3\alpha}, \tag{12a}$$

and

$$\beta_0 = B'\left(1 - \frac{e\mu}{3\sigma}\right). \tag{12b}$$

The value of B' $(0 < B' < 3)$ should be approximately 1.5 for the brightness of the resulting picture to be comparable with that of pictures having an average brightness of 0.5 for each of the three primary color components. Also, with this transformation the darkest and brightest pixels are assigned $(1 - e)$ and $(1 + e)$ times the average brightness $(0 \le e \le 1)$. The ratio $m = (1 + e)/(1 - e)$ is similar to the "lighting ratio," a term used to describe the ratio of main light to fill-in light in photography [14]. A higher e yields a wider range in brightness. The e value yielding the same brightness proportion as the original data is given as

$$e = \frac{3\sigma}{\mu}.$$

Thus, the brightness range is expanded and compressed for $e > 3\sigma/\mu$ and for $e < 3\sigma/\mu$, respectively. Since the hues of very dark or very bright spots on the picture are difficult to discriminate, values of $e = 0.5$ or $m = 3$ (the brightest and darkest ratios of 3) generally provide the best results for color photography [14]. Determination of B' and e will be described later.

The coefficients α_1 and β_1 are determined as follows. Since a pixel with no greenness ($y_2 = 0$) should look white (colorless), β_1 is determined to be 1/3. (For a colorless pixel we have $q_1 = q_2 = q_3 = 1/3$, regardless of brightness.) The coefficient α_1 is determined from the distribution of y_2/y_1, which may be obtained from the given image

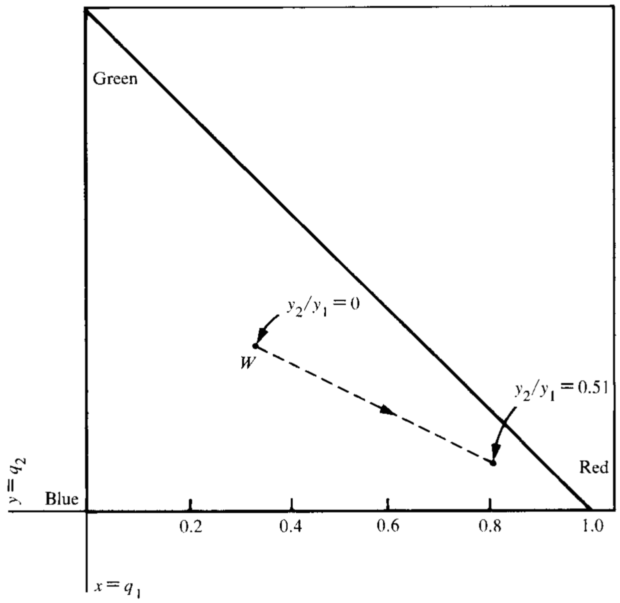

Figure 2 The transform $q_1 = f_1(y_2/y_1)$ shown on a chromaticity diagram.

or from a large collection of image data. If the latter is used, the red saturation level will be consistent among images represented by the collection of image data. In either case, we identify a level, $y_2/y_1 = d$, which is mapped to a red saturation level denoted by s. (Such d may be obtained at a level that contains the top one percent population of the y_2/y_1 distribution.) Therefore, α_1 is given as

$$\alpha_1 = \frac{s - 1/3}{d}. \tag{13}$$

In our example, the value obtained, $d = 0.51$, was based upon 58 subframes, and s was set equal to 0.8; the resulting transform from y_2/y_1 to q_1 is shown on a chromaticity diagram (Fig. 2). This figure shows a triangle whose three corners represent the trichromatic coefficients of blue, green, and red color guns in the chromaticity diagram given in Fig. 1.

In summary, if a color picture is generated from the first two components y_1 and y_2, the intensities of color modulation p_1, p_2, and p_3 are given from Eqs. (6), (11), and (12) as

$$p_1 = B'\left(\frac{e}{3\sigma}\, y_1 + 1 - \frac{e\mu}{3\sigma}\right)\left(\frac{3s - 1}{3d}\right)\left(\frac{y_2}{y_1}\right), \tag{14a}$$

$$p_2 = B'\left(\frac{e}{3\sigma}\, y_1 + 1 - \frac{e\mu}{3\sigma}\right) \times \left\{\frac{1}{2}\left[1 - \left(\frac{3s - 1}{3d}\right)\left(\frac{y_2}{y_1}\right)\right]\right\}, \tag{14b}$$

May 4, 1976 — July 15—16, 1976

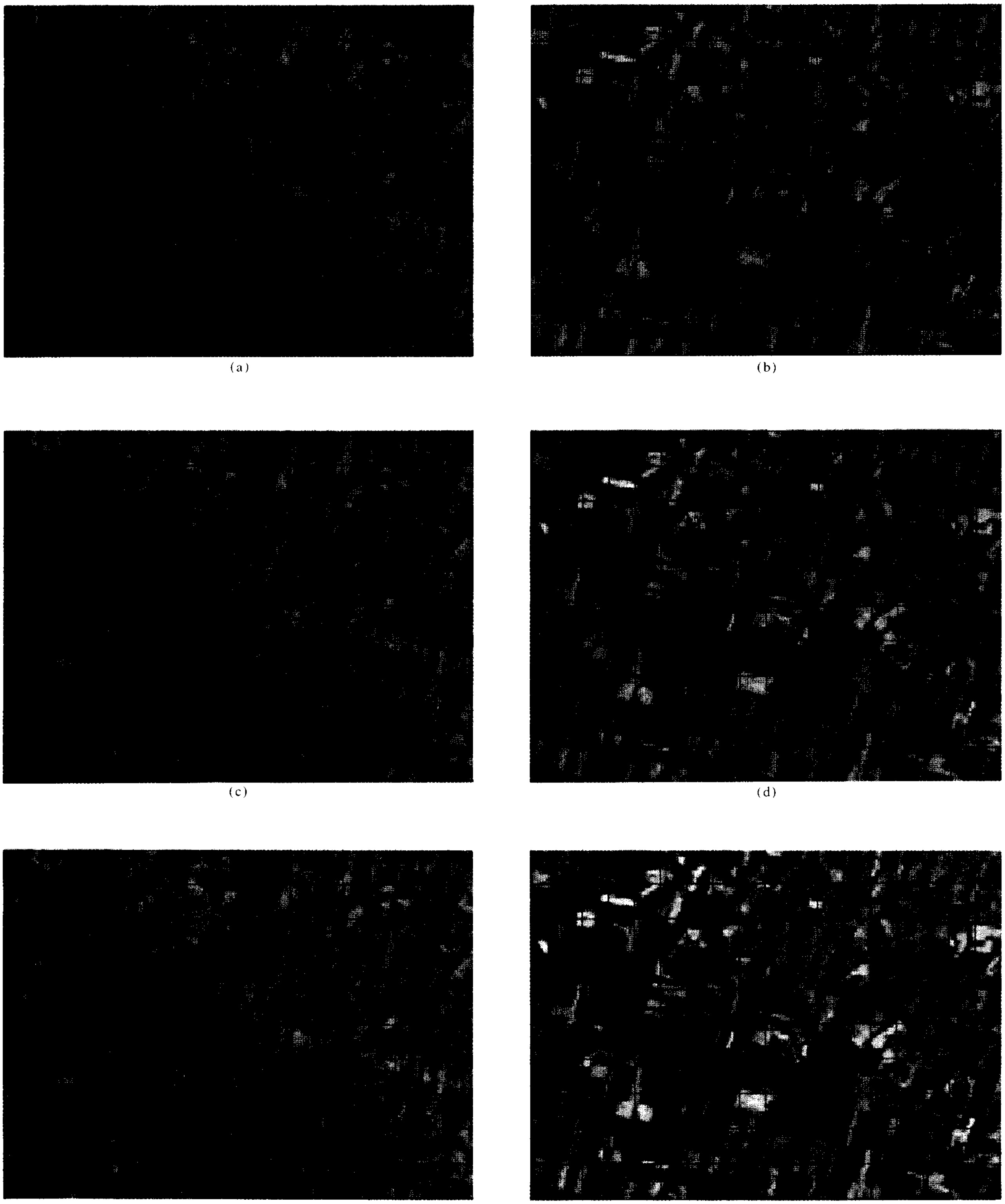

Figure 3 Comparison of color pictures made from principal components of MSS data with conventional color infrared pictures for a Nebraska site on different dates; image area is approximately 9×11 km^2; (a) and (b) from components y_1 and y_2, (c) and (d) from components y_1, y_2, and y_3, (e) and (f) conventional infrared pictures.

and

$$p_3 = p_2. \tag{14c}$$

In the above equations, e and B' are undetermined.

Now consider determining e and B'. Note that e and B' may be chosen freely as long as the conditions $0 \le p_1 \le 1$ and $0 \le p_2 \le 1$ are met. Since the second factor of Eq. (14a), $[(3s - 1)/3d](y_2/y_1)$, has a value between 0 and 0.8, the value of the second factor of Eq. (14b), $1/2\{1 - [(3s - 1)/3d](y_2/y_1)\}$, must be less than 0.5, and if

$$B' \left(\frac{e}{3\sigma} y_1 + 1 - \frac{e\mu}{3\sigma} \right) < 2, \tag{15}$$

the inequality $p_2 \le 1$ always holds. This inequality is satisfied by $e = 0.5$ and $B' = 1.33$. Although all of the inequalities given in Eq. (14) can be satisfied by reducing B', a value of B' smaller than 1 is not desirable because the resulting picture becomes dark. The most desirable value of B' is 1.5, as shown by the fact that B equals the average of $(p_1 + p_2 + p_3)$. Generally, we may choose one of the following policies:

a. Use fixed B' (e.g., 1.2) and fixed e (e.g., 0.5 or $3\sigma/\mu$).

b. Use fixed B' (e.g., 1.2) and variable e to satisfy $0 \le p_1, p_2, p_3 \le 1$.

The policy that should be adopted depends upon the requirements for color pictures. If brightness information is not important for a particular application, use of the smaller e is recommended. If $e = 0$, the brightness of every pixel is identical, and the resulting picture is called isoluminous. In this case, B' is set as

$$B' = \min \left[0.5, \frac{3d}{D(3s - 1)} \right], \tag{16}$$

where D is the level over which the top, say one percent, population is contained.

For a more general case, reasonable values of B' and e are chosen first. The maximum percentage of overloading for the 58 subframes taken for this experiment was six percent, with $B' = 1.2$ and $e = 0.5$.

- *Image generation by y_1, y_2, and y_3*

When three components y_1, y_2, and y_3 are used for generating a color picture, one more linear equation is added:

$$q_2 = \alpha_2 \frac{y_3}{y_1} + \beta_2. \tag{17}$$

Therefore, q_3 is set as

$$q_3 = 1 - q_1 - q_2, \tag{18}$$

where q_1 is given in Eq. (10). Since the white (or colorless) point should correspond to $y_2 = y_3 = 0$, $\beta_2 = 1/3$ is derived. The value of α_2 is chosen to be the same as α_1. With this choice for α_2, a unit change in y_2 and y_3 yields the same change in p_1 and p_2, respectively. If the range of y_3 is considerably smaller than that of y_2, a value of α_2 that is larger than α_1 may be chosen to enhance the change in y_3. For the 58 subframes studied, the standard deviations of y_2 and y_3 were 0.112 and 0.048, respectively. Therefore, with $\alpha_2 = \alpha_1$, the change in green and blue is about 40 percent of the change in red.

Since α_2 is taken to be positive, an increase in y_3 means an increase in q_2, i.e., a brightness increase for green. Therefore, picture elements (pixels) with larger y_2 and y_3 appear yellowish. This is in agreement with the phenological interpretation of y_3 (that y_3 represents yellowness).

- *Examples*

A pair of color films for the 58 acquisitions under investigation were generated with the photographic film converter at the NASA Johnson Space Center, Houston, TX. Color prints made from their negatives are shown in Figs. 3(a–d).

One was generated from y_1 and y_2 [Fig. 3(a)]; the other from y_1, y_2, and y_3 [Fig. 3(c)]. For both cases all the parameters were set the same: $B' = 1.2$, $e = 0.5$, and $\alpha_1 = \alpha_2 = 0.88$. With this setting, the distribution of p_1, p_2, and p_3, which control the brightness of red, green, and blue guns, was monitored. It was found that in both cases overloading took place only on the red gun. The highest frequency of overloading was six percent.

Figures 3(a) and 3(c) are color pictures generated from the first two and first three components, respectively, for an area of approximately 9×11 km^2 in Nebraska (acquired on May 4, 1976). These two pictures look very similar; however, Figs. 3(b) and 3(d), made from the first two and first three components, respectively, over the same site (but acquired on July 16, 1976) appear slightly different. Rectangular winter wheat fields that appear white in Fig. 3(b) look yellowish in Fig. 3(d), because matured or post-harvest wheat fields usually have a larger third component y_3.

Color infrared pictures made on May 4 and July 15, 1976, by a conventional method are shown in Figs. 3(e) and (f), respectively. These pictures were made by controlling the red, green, and blue guns with channel-4, -2, and -1 image data, respectively. Fields with vegetation (green) appear red in these pictures. The similarity of Figs. 3(a, c, and e) and Figs. 3(b, d, and f), respectively, is notable. Therefore, interpretation techniques based upon color infrared films that were obtained by using such conventional methods may be applicable to color infrared films that are made with the method presented here.

Summary

It is well known that the bands of an MSS, particularly the reflective bands (i.e., visible and near-infrared bands), are positively and highly correlated with one another. The number of useful bands can often be reduced by two to three if a principal axis transform is used. The first component of a principal axis transform is generally given as a weighted sum of all the channel responses. Since each channel response measures incoming energy, it is natural to associate the first component with brightness.

With this interpretation, a color picture generation method that controls the brightness with only the first component has been presented. This method is different from those presented by previous workers [10, 11], in which all three components are used for controlling any one gun, blue, green, or red. With their methods, the brightness, for instance, of the resulting picture depends upon all of the first three components. Pictures produced by these other methods appear very different from conventional infrared pictures, and require the development of a new photo-intepretation technique. On the other hand, pictures made by the method described in this paper are remarkably similar to conventionally made pictures. In conclusion, this method has the distinct advantage of being able to present almost all of the information in an MSS image form compatible with conventional color infrared pictures.

Acknowledgments

The author expresses appreciation to P. N. Misra for helpful discussions during the initial formulation of the problem, and to S. K. Tinkler of the NASA Johnson Space Center, Houston, TX, for help in obtaining color infrared films. This work was supported by the NASA Johnson Space Center under Contract No. NAS9-14350.

References and note

1. R. G. Reeves, A. Anson, and D. Landen, eds., *Manual of Remote Sensing*, American Society of Photogrammetry, Falls Church, VA, 1975.
2. Committee on Remote Sensing for Agricultural Purposes. Agricultural Board, National Research Council, *Remote Sensing, with Special Reference to Agriculture and Forestry*, National Academy of Sciences, Washington, DC, 1970.
3. S. Wenderoth and E. Yost, *Multispectral Photography for Earth Resources*, Long Island University, Greenvale, NY, prepared for the NASA Johnson Space Center, Houston, TX.
4. F. Johnson, "Graphic Study of Corn and Soybean Data," part 5 of *Crop Identification Technology Assessment for Remote Sensing (CITARS)*, Vol. VIII, JSC 09391, NASA Johnson Space Center, December 1975.
5. R. J. Kauth and G. S. Thomas, "The Tasselled Cap—A Graphic Description of the Spectral-Temporal Development of Agricultural Crops as Seen by LANDSAT," *Proceedings of the 1976 Machine Processing of Remotely Sensed Data Symposium*, Purdue University, IN, June 29–July 1, 1976, p. 4B–41.
6. S. G. Wheeler and P. N. Misra, "Linear Dimensionality of LANDSAT Agricultural Data with Implications for Classification," *Proceedings of the 1976 Machine Processing of Remotely Sensed Data Symposium*, Purdue University, IN, June 29–July 1, 1976, p. 2A–1.
7. G. J. McMurtry and F. Y. Borden, "Principal Components and Canonical Analysis for Skylab Channel Evaluation," *Proceedings of the 1977 Machine Processing of Remotely Sensed Data Symposium*, Purdue University, IN, June 21–23, 1977, p. 77.
8. S. G. Wheeler and R. H. Wolfe, Jr., IBM/FSD, Houston, TX, private communication.
9. P. J. Ready and P. A. Wintz, "Information Extraction, SNR Improvement, and Data Compression in Multispectral Imagery," *IEEE Trans. Commun.* **COM-21,** 1123 (1973).
10. A. Fontanel, C. Blanchet, and C. Lallemand, "Enhancement of LANDSAT Imagery by Combination of Multispectral Classification and Principal Component Analysis," *Proceedings of the NASA Earth Resources Survey Symposium*, Houston, TX, 1975, p. 991.
11. A. Santisteban and L. Munoz, "Application of Image Principal Component Technique to the Geological Study of a Structural Basin in Central Spain," *Proceedings of the 1977 Machine Processing of Remotely Sensed Data Symposium*, Purdue University, IN, June 21–23, 1977, p. 228.
12. K. Fukunaga, *Introduction to Statistical Pattern Recognition*, Academic Press, Inc., New York, 1972.
13. Linear functions are chosen here for their simplicity, but other functions may be used to emphasize or de-emphasize particular domains, depending upon the application.
14. "Color as Seen and Photographed," *Kodak Publication No. E74*, Eastman Kodak Company, Rochester, NY.

Received September 13, 1977; revised February 17, 1978

The author is with the IBM Federal Systems Division, 1322 Space Park Drive, Houston, Texas 77058.